Effect of electric field on one-dimensional insulators: a density matrix renormalization group study

2007 J. Phys.: Condens. Matter 19 322201

(http://iopscience.iop.org/0953-8984/19/32/322201)

IOP FTC

IOP PUBLISHING JOURNAL OF PHYSICS: CONDENSED MATTER

J. Phys.: Condens. Matter **19** (2007) 322201 (7pp) doi:10.1088/0953-8984/19/32/322201

FAST TRACK COMMUNICATION

Effect of electric field on one-dimensional insulators: a density matrix renormalization group study

Sudipta Dutta, S Lakshmi and Swapan K Pati

Theoretical Sciences Unit and DST Unit on Nanoscience, Jawaharlal Nehru Centre for Advanced Scientific Research, Jakkur Campus, Bangalore 560064, India

Received 23 April 2007
Published 27 June 2007
Online at stacks.iop.org/JPhysCM/19/322201

Abstract

We perform density matrix renormalization group (DMRG) calculations extensively on one-dimensional Mott and Peierls chains with explicit inclusion of the static bias to study the insulator–metal transition in those systems. We find that the electric field induces a number of insulator–metal transitions for finite-size systems and, at the thermodynamic limit, the insulating system breaks down into a completely conducting state at a critical value of bias that depends strongly on the insulating parameters. Our results indicate that the breakdown, in both the Peierls and Mott insulators, at the thermodynamic limit, does not follow the Landau–Zener mechanism. Calculations on various size systems indicate that an increase in the system size decreases the threshold bias as well as the charge gap at that bias, making the insulator–metal transition sharper in both cases.

Strongly correlated low-dimensional electronic systems have attracted much interest because of their unique low-energy characteristics [1–5]. These systems are almost always insulators due to various interactions in reduced dimensions and are commonly described by Hubbard, Peierls or related Hamiltonians [6, 7]. While the ground state of a half-filled Hubbard system is a Mott insulator, the electron–lattice interactions lead to Peierls instability in low-dimensional systems.

The effect of an electric field on such systems has generated much interest in recent years due to the practical interest in tuning their dielectric and piezoelectric properties, more so for the Mott insulators. Many electronic conduction processes seem to suggest electric-field-induced phenomena, such as negative differential resistance in molecular electronics [8, 9]. Recent experiments on low-dimensional Mott insulators, namely Sr_2CuO_3, $SrCuO_2$ [10] and $La_{2-x}Sr_xNiO_4$ [11] suggest a dielectric breakdown in the presence of an external electric field. While the Peierls case is relatively easy, a tractable computational method which takes into account the static electric field and its response on the excited correlated electronic states is still lacking. One of the earliest theoretical approaches considering an electric field was the Bethe-*ansatz* method [12, 13], where asymmetric tunnelling terms towards the left and right were considered in order to describe the non-equilibrium situation and hence capture the flavour of

an electric field. However, the imaginary gauge term giving rise to a non-hermitian Hamiltonian makes it very difficult to relate this to a system in the presence of a real electric field. In order to account for this, another approach to this problem has been to employ the time-dependent Schrödinger equation to study the time evolution of the many-body wavefunctions and levels, where the electric field is applied via a time-dependent Aharonov–Bohm flux [14]. However, in this case the calculations are restricted to only ring structures (to avoid ambiguities arising from the electrodes) and for system sizes of fewer than ten sites. Recently, however, there have been a number of studies using the real-time evolution of the ground state in the presence of a source drain potential [15]. However, a microscopic understanding of the insulator–metal transition and the quantification of the critical static electric field, required to induce it in real extended systems, is still lacking.

For a clear understanding of the effect of electric field on finite-size systems as well as in the thermodynamic limit, in this letter, we use the density matrix renormalization group (DMRG) method [16, 17] which is known to be highly accurate for low-dimensional interacting systems. For the first time, we have included a static electric field in the DMRG algorithm and have obtained ground and low-energy eigen-states of a one-dimensional system with various sizes. The static electric field is included as a ramp potential and we find that the electric field can induce a number of insulator–metal transitions for finite-size systems, with the transition depending on the Hamiltonian parameters. We analyse our results at the thermodynamic limit in the light of the Landau–Zener mechanism [18], for both the Peierls and Mott insulating systems. To get the thermodynamic behaviour we consider the total bias instead of the field.

We consider a one-dimensional chain representing a conjugated polymer or any other one-dimensional system, described by the Peierls–Hubbard Hamiltonian,

$$H = \sum_i (t + (-1)^{i+1}\delta)(a^\dagger{}_i a_{i+1} + \text{h.c}) + U \sum_i n_{i\uparrow} n_{i\downarrow}, \tag{1}$$

where t is the hopping term, U is the Hubbard term and δ is the bond alternation parameter. We set $t = 1$ and, for the Mott-insulator, we consider $\delta = 0$ and nonzero U, while, for the Peierls-insulator, U is set to zero with nonzero δ. The external electric field applied on the system has the form of a ramp potential, distributed over all the sites in such a way that the potential V_i at site i becomes $-\frac{V}{2} + i\frac{V}{N+1}$, where V is the applied voltage and N is the total number of sites in the 1D chain. This form of the potential ensures that the bias varies between $-V/2$ to $V/2$ across the molecule. The potential adds an extra term $\sum_i V_i a^\dagger{}_i a_i$ to the above Hamiltonian.

Our DMRG results compare fairly well with the $V = 0$ Bethe-*ansatz* ground-state energy and charge gap, for all values of U, with a density-matrix cut-off $m = 140$. For nonzero bias, the DMRG results compare up to numerical accuracies with the exact diagonalization results of finite sizes up to $N = 16$. For $U = 0$, the problem can be solved exactly and we obtain the ground state and excitation spectrum in the presence of bias using the tight-binding one-electron formalism. In the Mott (Peierls) case, where $U(\delta)$ has been varied from 0 to 5 (0 to 1) with bias from 0 to 6 V in steps of 0.1 V.

For many-body models, the charge excitation gap is defined as the difference between the energy required to add (μ_+) and remove (μ_-) electrons from the ground state [19],

$$\Delta_{\text{charge}} = \mu_+ - \mu_-, \tag{2}$$

where $\mu_+ = E(N+1) - E(N)$ and $\mu_- = E(N) - E(N-1)$. $E(N)$, $E(N+1)$ and $E(N-1)$ are the energies of the half-filled system and the systems with one extra and one less electron, respectively.

To understand the energy cost due to the addition or removal of electrons in the presence of bias, we have calculated μ_+ and μ_- numerically using DMRG for a range of biases. In

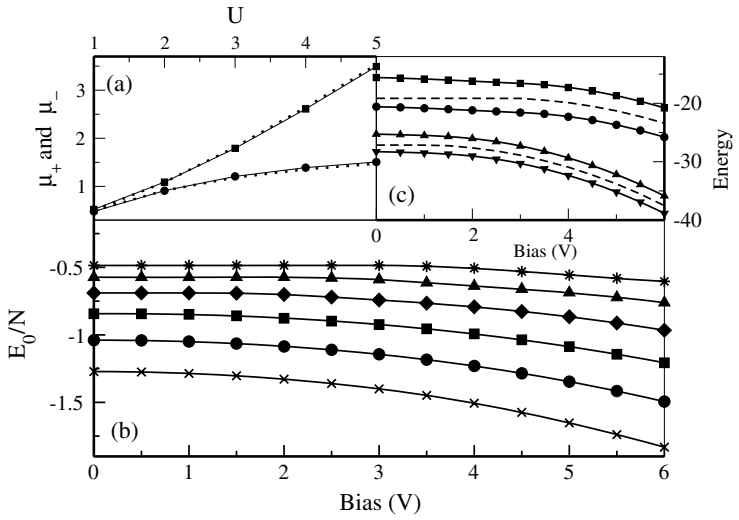

Figure 1. (a) $N \to \infty$ values of μ_+ (square) and μ_- (circle) at zero bias as a function of U. The dotted lines correspond to exact Bethe-*ansatz* results. (b) Converged ground-state energy per site $\frac{E_0}{N}$ for half-filled system (N electrons) versus applied bias (V) for $U = 0(X)$, 1 (circle), 2 (square), 3 (diamond), 4 (triangle) and 5 (star). (c) The energy of the systems with $N+1$ (up triangle (square)), and $N-1$ (down triangle (circle)) electrons for $U = 3(5)$ for a chain of 40 sites as a function of bias. The dashed lines represent the corresponding ground-state energy ($E(N)$).

figure 1(a), we have plotted μ_+ and μ_- as a function of U at zero bias. The finite-size DMRG results (μ_+ and μ_-) are extrapolated to the thermodynamic limit ($N \to \infty$) for every U value. For a clear demonstration of the accuracy of our results, we have also shown the Bethe-*ansatz* μ_+ and μ_- values derived for every U in the same plot. As can be seen, our numerical extrapolated values compare fairly well with the exact thermodynamic Bethe-*ansatz* results. Both μ_+ and μ_- increase with an increase in U. However, the former increases with larger slope than the latter, resulting in an increase in the charge gap with increasing Hubbard repulsion. This is because a higher value of Hubbard repulsion localizes the electrons more and leads to higher charge gap.

The ground state of the Hamiltonian with nonzero U is a spin-density wave insulator with one electron at every site [20]. In figure 1(b) we have plotted the converged (extrapolated value at the $N \to \infty$ limit) ground-state energy of the half-filled system as a function of applied bias for different U values. As can be seen, for a fixed U value, the ground-state energy remains almost constant up to a certain bias, and beyond it the system starts stabilizing rapidly with applied bias [21]. It can thus be interpreted from figure 1(b) that the applied electric field stabilizes the system after a threshold value, required to overcome the effect of the electron repulsion, U. Thereafter, the system gains kinetic energy as the electrons start hopping in the direction of bias. For $U = 0$, the stabilization starts as soon as the bias is turned on.

To understand the response of the excited states of the system with electric field, for a given U, we have computed $E(N+1)$ and $E(N-1)$. Both the energies for a particular system size ($N = 40$) are plotted in the figure 1(c) as a function of bias for two representative U values, together with $E(N)$. As for the ground state, the excitation energies (both $E(N+1)$ and $E(N-1)$) decrease with an increase in bias, however their difference always remains equal to U for all values of bias, as expected. For a given value of U, although the slopes of $E(N+1)$ and $E(N-1)$ are the same and the slope of $E(N)$ is different, leading to the interesting phenomenon

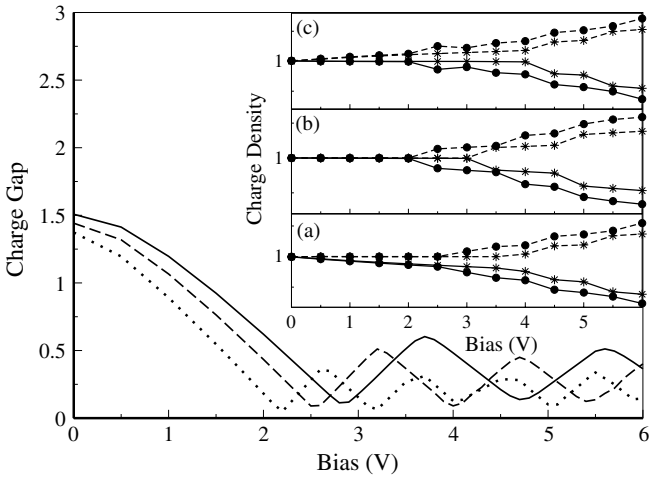

Figure 2. Charge gap versus bias for $N = 20$ (solid line), 26 (dashed line) and 40 (dotted line) for $U = 4$. Inset shows the charge densities on first site (solid lines) and last site (dashed lines) for the $N - 1$ (a), N (b) and $N + 1$ (c) electron systems as a function of bias for $U = 4$ (circle) and 5 (star) with $N = 30$.

of insulator–metal transition, as described later. Figure 1(c) also shows that stabilization of the system with one extra/less electron needs a higher bias for higher value of U.

To characterize accurately the bias at which this insulator–metal transition occurs, we plot in figure 2 the charge gap as a function of bias for different finite-size systems for a representative value of U. It can be seen clearly that the charge gap shows an oscillation with bias, going through a number of minima and maxima. To understand the underlying physics, we have calculated the on-site charge densities as a function of bias for various system sizes with several U values. We present this in the inset of figure 2 for the half-filled state and the states with one extra and one less electron than half-filling for two representative values of U for a finite chain with $N = 30$. For clarity, we plot charge densities at only the first and the last sites. At zero bias, the ground-state charge density at every site of the system is the same and it remains almost the same with an increase in bias up to the bias corresponding to the first minimum of the charge gap (ΔE). However, after that, they show a large shift in the direction of bias, giving rise to charge inhomogeneties. A higher value of U requires a higher bias to shift the charge density, as can be seen from the inset of figure 2 and thus the bias corresponding to the first ΔE minimum increases with increasing U. Interestingly, the repetetive period of charge gap going through minima with an increase in bias is due to the role of charge stiffness. The external bias tends to shift the charge densities towards one electrode with the nullification of U at the first ΔE minimum. However, beyond this, an increase in the bias results in further hopping of charges, leading to double occupancy of more sites, with electron repulsion overwhelming the kinetic stablization, thereby increasing the energy gap. A further increase in bias nullifies this effective repulsion, resulting in the next charge gap minimum. Hence, such a variation in the charge gap, resulting in a near-metallic behaviour (where the charge gap is not zero) in various bias regions, is due to the interplay of the Hubbard repulsion, finite system size and the spatial gradient of the external bias. Interestingly, as can be seen from figure 2, with an increase in the size, the magnitude of bias corresponding to the first ΔE minimum reduces and the periodicity of the occurence of succesive minima thereafter also narrows down. The field (V/N) required to reach the first ΔE minimum decreases more sharply with an increase in system size.

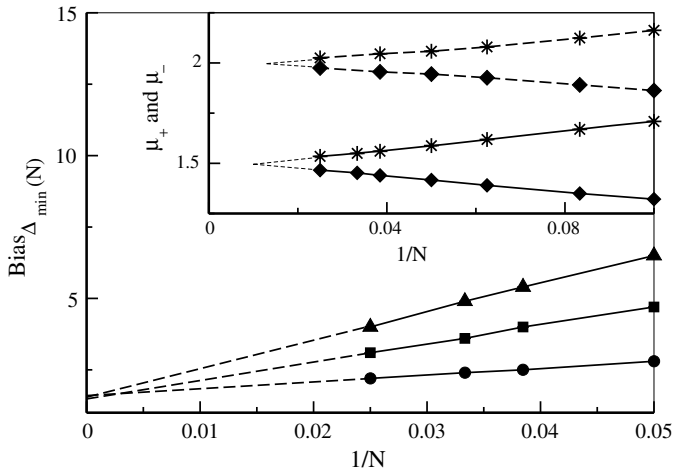

Figure 3. Bias at first (circle), second (square) and third (triangle) minima as a function of $1/N$ for $U = 4$. Dashed lines show the extrapolation. Inset shows the μ_+ (star) and μ_- (diamond) at the first minimum as a function of $1/N$ for $U = 3$ (solid lines) and 4 (dashed lines). Dotted lines are extrapolation. Error bars are of the same size as the symbols.

To explore the size dependence of this insulator–metal transition, in figure 3 we plot the bias values corresponding to the first, second and third ΔE minima separately as a function of $1/N$ and extrapolate the plots to the $N \to \infty$ limit. All the minima converge to the same point at the thermodynamic limit, clearly indicating that, at the $N \to \infty$ limit, the system goes to a conducting state at some bias which we term the critical bias, V_c. At this V_c, the ground state of the system changes its slope and starts stabilizing rapidly, as can be seen from figure 1(a). In the inset of figure 3, we show μ_+ and μ_- at the first minimum as a function of inverse system size for $U = 3$ and 4. With an increase in system size, μ_+ and μ_- come close to each other and thus the gap at the first minimum becomes smaller with larger deconfinement. From our finite-size data analysis, with extrapolation to the $N \to \infty$ limit, we find that, with an increase in the Hubbard repulsion term, U, the difference between μ_+ and μ_- at the first minimum for a particular finite chain decreases, as can be seen from the inset. Thus with an increase in U, the length of the chain at which the charge gap vanishes decreases. Hence, as is evident from the inset, for a given value of U, our method enables us to predict the length of the chain at which the system will become completely conducting.

It is clear from the above discussion that the bias required for the closing of the Mott gap depends sensitively on the value of U. To understand how V_c depends on U, in figure 4 we plot V_c as a function of U obtained from our calculations, along with that calculated using the Landau–Zener formula [22] on the initial charge gaps obtained using the Bethe-*ansatz*. Figure 4 shows a nonlinear dependence of V_c on U. We have also analysed the insulator–metal transition in the case of Peierls insulators. In this case, the difference between the highest occupied and lowest unoccupied single-electron states (opposite parity) is the charge gap. Here, too, the critical bias has a sensitive dependence on the bond-alternation parameter, δ, as has been described previously by us [23, 24]. The inset of figure 4 displays the variation in converged V_c with δ. To now compare and contrast the critical bias obtained for the Peierls and Mott insulators in the light of the Landau–Zener formula, we analyse the initial charge gap and the V_c dependence on the model parameters, δ and U. For Peierls insulators, the $V = 0$ charge gap is linear in δ, and the critical bias V_c, calculated at the thermodynamic limit (inset in figure 4)

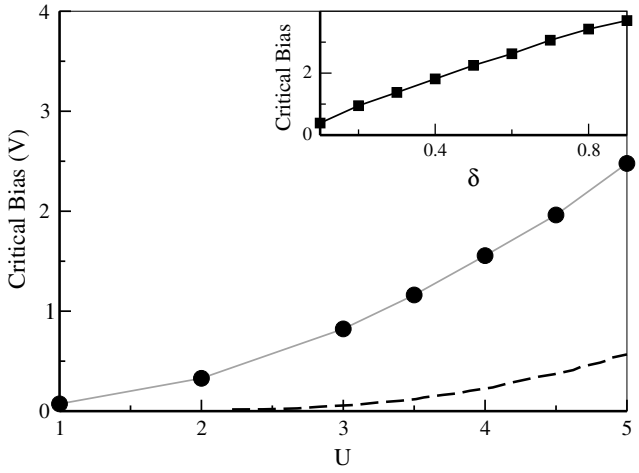

Figure 4. V_c as a function of U from our results (circle) and the Bethe-*ansatz* prediction of Landau–Zener tunnelling (dashed line). Inset shows V_c as a function of δ.

has a near linear dependence on δ. This indicates that the Landau–Zener formula, which has the form $V_c(\delta) \propto [\Delta_{\text{charge}}(\delta)]^2$, is not obeyed, although previous studies on finite-size systems indicated that tunnelling occurs between the Landau quasi-degenerate valence and conduction levels [23–25], resulting in an exchange of their symmetries. This is because, at the large-N limit, the gap at the critical bias goes to zero and the system goes to a completely conducting state. In the case of the Mott insulator, the initial charge gap has a nonlinear dependence on U and, as seen in figure 4, the critical bias also shows a nonlinear dependence on U. A fitting gives $V_c(U) \propto [\Delta_{\text{charge}}(U)]^n$, with $n \sim 1$, which, unlike the results from previous studies [22], clearly indicates that the tunnelling between many-body levels does not follow the Landau–Zener mechanism in the thermodynamic limit. Note that, in our case, V_c corresponds to the total bias applied to the chain with $N \to \infty$, while the time-dependent studies [22, 25] calculate the critical field (V_c/N) by converging it up to a certain finite chain length. We do not consider the effect of polarization on the applied electric field in our calculations because the inclusion of polarization does not change the nature of the insulator–metal transition, as we have observed earlier [23]. It can only change the quantitaive estimation of the bias at charge gap minima to some extent. Moreover, in the presence of the Hubbard repulsion term U, the ramp nature of the electric field is retained, even with the inclusion of polarization effects in our calculations [26].

Qualitatively, the change in slope of the ground state can be visualized even for a two-sites Mott-insulating system. For $V = 0$, the ground state of the half-filled system consisting of four basis states has a large contribution from the singly occupied sites, with a second-order (t^2/U) contribution from the double-occupancy sites. However, the external bias nullifies the Hubbard repulsion, leading to a mixing of the double-and single-occupancy sites. The ground-state charge density shifts in the direction of the applied electric field, at $V \sim 3U$. On the other hand, the state with one extra electron consisting of two basis states stabilizes with a slope that does not depend on U. This is because the external bias results in the hopping of an electron from one site to another, leading to a preference for one of the basis states compared to the other. But, since both basis states are energetically degenerate, this hopping occurs without any Hubbard energy cost; rather, the energy decreases due to kinetic stabilization. This results in a slope that is independent of the Hubbard repulsion. Additionally, the Hubbard repulsion also

does not play any role in the two-sites one-electron case. The two-sites problem thus captures the ground-state behaviour, and not the transition pheonomena, since the interesting features described earlier (ΔE oscillation) leading to breakdown behaviour occur primarily due to the response of the excited states to an applied static electric field.

In conclusion, we have shown that, in the thermodynamic limit, the insulator–metal transition in the presence of an external static electric field does not follow the Landau–Zener mechanism in both Peierls and Mott insulators. Our DMRG calculation is the first of its kind, which allows us to study various system sizes with a better understanding of the general insulator–metal transition, with quantitative predictability.

SD acknowledges the Council of Scientific and Industrial Research (CSIR) for the research fellowship and SKP acknowledges research support from Department of Science and Technology and CSIR, the Government of India.

References

[1] Geller Michael R 2001 *Preprint* cond-mat/0106256
[2] Torrance J B, Vazquez J E, Mayerle J J and Lee V Y 1981 *Phys. Rev. Lett.* **46** 253
Del Freo L, Painelli A and Soos Z G 2002 *Phys. Rev. Lett.* **89** 027402
Anusooya Y, Soos Z G and Painelli A 2001 *Phys. Rev.* B **63** 205118
[3] Dagotto E 2005 *Science* **309** 257
Yanase Y *et al* 2003 *Phys. Rep.* **387** 1
[4] Wiegmann P B 1988 *Phys. Rev. Lett.* **60** 821
[5] Ogota M and Anderson P W 1993 *Phys. Rev. Lett.* **70** 3087
[6] Gutzwiller M C 1963 *Phys. Rev. Lett.* **10** 159
Hubbard J 1963 *Proc. R. Soc.* A **276** 238
Hubbard J 1964 *Proc. R. Soc.* A **277** 237
[7] Su W P, Schreiffer J R and Heeger A J 1979 *Phys. Rev. Lett.* **42** 171
Su W P, Schreiffer J R and Heeger A J 1980 *Phys. Rev.* B **22** 2099
[8] Chen J, Reed M A, Rawlett A M and Tour J M 2001 *Science* **286** 1550
Chen J, Reed M A, Rawlett A M and Tour J M 2000 *Appl. Phys. Lett.* **77** 1224
[9] Lakshmi S and Pati S K 2005 *Phys. Rev.* B **72** 193410
[10] Taguchi Y, Matsumoto T and Tokura Y 2000 *Phys. Rev.* B **62** 7015
[11] Yamanouchi S, Taguchi Y and Tokura Y 1999 *Phys. Rev. Lett.* **83** 5555
[12] Fukui T and Kawakami N 1998 *Phys. Rev.* B **58** 16051
[13] Deguchi T *et al* 1998 *J. Phys. A: Math. Gen.* **31** 7315
[14] Oka T, Arita R and Aoki H 2003 *Phys. Rev. Lett.* **91** 066406
[15] Al-Hassanieh K A *et al* 2006 *Phys. Rev.* B **73** 195304
Schneider G and Schmitteckert P 2006 *Preprint* cond-mat/0601389
[16] White S R 1992 *Phys. Rev. Lett.* **69** 2863
White S R 1993 *Phys. Rev.* B **48** 10345
[17] Schollwöck U 2005 *Rev. Mod. Phys.* **77** 259
Pati S K, Ramasesha S and Sen D 2003 *Magnetism: Molecules to Materials IV* ed J S Miller and M Drillon (Weinheim: Wiley–VCH) p 199
Lakshmi S, Datta A and Pati S K 2005 *Phys. Rev.* B **72** 045131
[18] Landau L D 1932 *Phys. Z. Sowjetunion.* **2** 46
Zener C 1932 *Proc. R. Soc.* A **137** 696
Stückelberg E C G 1932 *Helv. Phys. Acta* **5** 369
[19] Lieb E H and Wu F Y 1968 *Phys. Rev. Lett.* **20** 1445
[20] Campbell D K, Baeriswyl D and Majumdar S 1992 *Conjugated Conducting Polymers* (*Springer Series in Solid-State Science* vol 102) ed H Kiess (New York: Springer)
[21] Souza I, Iniguez J and Vanderbilt D 2002 *Phys. Rev. Lett.* **89** 117602
[22] Oka T and Aoki H 2005 *Phys. Rev. Lett.* **95** 137601
[23] Lakshmi S and Pati S K 2004 *J. Chem. Phys.* **121** 11998
[24] Sengupta S, Lakshmi S and Pati S K 2006 *J. Phys.: Condens. Matter* **18** 9189
[25] Oka T, Arita R and Aoki H 2005 *Physica* B **359** 759
[26] Lakshmi S and Pati S K 2003 *Proc. Indian Acad. Sci.* **115** 533